ELSEVIER

Surface and Coatings Technology 146–147 (2001) 250–257

SURFACE & COATINGS TECHNOLOGY

www.elsevier.com/locate/surfcoat

Structure and properties of novel functional diamond-like carbon coatings produced by laser ablation

Q. Wei[a,*], J. Sankar[a], J. Narayan[b]

[a]*NSF Center for Advanced Materials and Smart Structures, Department of Mechanical Engineering, North Carolina A&T State University, 1601 E. Market Street, Greensboro, NC 27411, USA*

[b]*Department of Materials Science and Engineering, Burlington Labs, P.O. Box 7916, North Carolina State University, Raleigh, NC 27695-7916, USA*

Abstract

Diamond-like carbon (DLC) mainly consists of sp^3 bonded carbon atoms. It can have properties that rival those of crystalline diamond. Its beneficial properties stem from the continuous rigid random networks of sp^3 carbon atoms, and the properties can essentially be tailored by the sp^3/sp^2 ratio. DLC coatings or thin films can be prepared by pulsed laser ablation (PLA), filtered cathodic vacuum arc (FCVA) deposition and mass selected ion beam (MSIB) deposition. In the past decade, tremendous progress has been made in experimental and theoretical investigations of hydrogen-free DLC. Experimental and commercial applications in microelectronics, micro-tribology, biomedical technologies, etc., have been demonstrated. Potential applications include sensors, flat panel displays (field emitters), photodiode, etc. In this paper, we report comprehensively the past and recent efforts in the research of functional diamond-like carbon coatings prepared by pulsed laser ablation in our group. In order to alleviate the internal compressive stress problem associated with high quality DLC coatings, we have adopted a novel and simple target design. The films were characterized by Raman spectroscopy, transmission electron microscopy, IR range optical measurements, tribological measurement, etc.

Keywords: Diamond-like carbon; Pulsed laser deposition; Functional materials

1. Introduction

The range of different forms of carbon, such as crystalline diamond, graphite, fullerenes, nanotubes, and amorphous carbon, etc., has made carbon one of the most fascinating elements in nature [1]. The great variety of structures and the unique properties of carbon are a result of its capability of forming various bonding states [2], e.g. tetrahedral (sp^3), trigonal (sp^2) and linear (sp^1) bonding. Diamond-like carbon (DLC) is an important form of amorphous carbon consisting of a mixture of sp^3 and sp^2 coordination. The beneficial properties of DLC are due to the sp^3 constituents that make DLC mechanically hard, infrared (IR) transparent, and chemically inert [3]. High quality DLC coatings can rival crystalline diamond in terms of mechanical performance (the hardness of crystalline diamond is approx. 100 GPa, its Young's modulus being approx. 1000 GPa) [4]. Furthermore, unlike polycrystalline diamond coatings prepared by chemical vapor deposition (CVD) and other techniques, DLC coatings are synthesized at much lower temperatures and are extremely smooth. Because of their advantageous properties, DLC coatings have found applications as hard protective coatings for magnetic disk drives, as antireflective coatings for IR windows, as field emission source for emitters, etc. [5–7].

It has been corroborated that ultraviolet (UV) pulsed laser ablation (PLA) of a high purity graphite target is able to produce high quality DLC films with a Tauc gap of $\sim$1.0–2.0 eV and an sp^3/sp^2 ratio up to 80% [8–10]. The interesting aspect of PLA is that it is a non-

* Corresponding author. Current address: Department of Mechanical Engineering, The Johns Hopkins University, North Charles Street, Baltimore, MD 21218, USA. Tel.: +1-410-516-5162.

E-mail address: qwei@pegasus.me.jhu.edu (Q. Wei).

0257-8972/01/$ - see front matter
PII: S0257-8972(01)01394-9

equilibrium process and the species produced in the laser plasma possess very high kinetic energy. For example, the kinetic energy of atomic species produced by electron beam evaporation is approximately $\sim kT$ ($\sim$0.025 eV at ambient temperature) (k is the Boltzmann constant and T is the absolute temperature) whereas those produced by pulsed laser may be as high as 100–4000 kT ($\sim$2.5–100 eV) [11,12]. More than one target can be loaded into the target carousal in an experiment, which enables one to tailor the chemical composition of the deposited films quite well. Upon optimization, PLA produces DLC coatings superior to filtered cathodic vacuum arc (FCVA) deposition [13] and mass selected ion beam (MSIB) deposition [14].

Successful preparation and application of DLC films have long suffered by a large internal compressive stress as high as 10 GPa [13] in the films regardless of the film growth technique employed [15–17]. Explanation for the presence of this stress is based upon the subplantation mechanism of DLC deposition. In this mechanism, incident energetic carbon species bombard the existing DLC film and since usually it takes place at room temperature where mobility of atoms is quite limited, it will give rise to a large compressive stress [15,18]. McKenzie et al. [19] even argued that a large compressive stress is a prerequisite for the formation of high quality DLC films. Adhesive failure of the coating may occur when the internal stress exceeds a critical value, which sets the upper limit on the coating thickness.

Traditional approaches to obtaining DLC coatings with reduced internal stress levels involve increasing deposition temperatures or decreasing the energies of carbon species arriving at the substrate surface, etc. All these are achieved at the expense of reducing the sp^3/sp^2 ratio. Some efforts have also been directed toward improving the adhesion of DLC films by depositing an interlayer or several interlayers between the DLC film and the substrate [20–22]. Recently, Friedmann et al. [23] reported preparation of thick stress-free DLC films (up to 1.2 μm thick) with hardness near that of diamond by PLD via a post-deposition annealing route. Ferrari et al. [24] reported a study of the stress release and structural changes caused by post-deposition annealing of DLC on Si produced by FCVA deposition. The advantage of thermal annealing is that pure DLC films can be prepared. One of the disadvantages is that throughput is largely decreased, and for microelectronic applications the thermal budget may become a great concern. Another apparently successful route to address the internal compressive stress associated with DLC coatings is by incorporation of more compliant atoms into the coatings [25–30].

In this paper, we present our studies on the structure and properties of functional DLC coatings prepared by PLA. To address the internal stress issue, we have adopted a modified target configuration so as to in situ incorporate foreign atoms into the DLC coatings during PLA. To further enhance the adhesion and increase coating thickness, we apply functionally graded design by manipulating the content of the foreign elements as a function of the distance from the DLC/substrate interface. This allows us to process DLC coatings as thick as 1.5 μm with strong adhesion to the substrate. Visible Raman spectroscopy, X-ray photon spectroscopy (XPS), Rutherford backscattering spectrometry (RBS), transmission electron microscopy (TEM) and radial distribution function (RDF) analysis, and optical microscopy were used to acquire structural information on the deposited coatings. The tribological behavior of the coated specimens was assessed by wear test and qualitative scratch test (for adhesion assessment) and depth sensing nanoindentation. Physical properties such as electric conduction, temperature-conduction behavior, and light effect on the conduction, as well as IR range optical properties, etc., are also reported. The results were interpreted based on a preliminary model.

2. Experimental procedure

2.1. Materials and pulsed laser ablation

The target configuration was described elsewhere [27]. Briefly, the graphite target was partly covered by a dopant piece. During PLA, the target was spinning and the focused laser beam impinges sequentially on graphite and the dopant portions to ablate the target materials to form a composite film. In order to apply the functionally graded design, four targets were loaded into the target carousal, one of which is pure graphite and the other three were partly covered by different size of dopant pieces. The p-type silicon (100) wafers were used as substrates, which were cleaned by a standard method to remove the native oxide layer before loading into the laser deposition chamber. Copper, silver, titanium and silicon were chosen as dopants, because a copper interlayer between the substrate and a DLC film has been demonstrated to improve the adhesion of the film. Ti is a strong carbide former, and Si is carbide former with covalent (sp^3) bonding similar to diamond.

The laser source used was pulsed KrF excimer laser ($\lambda_s = 248$ nm, duration time at half-maximum $\tau_s = 25$ ns) at a repetition rate of 10 Hz, which gives an energy density close to 3.0 J/cm^2. All the depositions were conducted at room temperature. The deposition chamber was evacuated to a base vacuum of approximately 1×10^{-7} torr by a turbo molecular pump with a mechanical pump.

2.2. Characterization of the DLC coatings

The thickness of the coatings was measured by a profilometer. The surface morphology of the films was

investigated using optical microscopy. Raman spectra were collected using a 514.7-nm laser beam and were decomposed into two Gaussians to study the peak shift so as to get information on the bonding characteristics and the internal stress reduction. Both RBS and XPS were used for chemical composition determination. The microstructure and atomic structure were studied using TEM. RDF analyses were performed to acquire information of short-range order of the DLC coatings.

Qualitative scratch tests were conducted on the specimens to study the adhesion of the DLC coatings to the substrate. The scratches were made under a constant normal load, and were observed and compared via optical microscopy. A 'crater grinding' method based upon micro-abrasion was used to measure the wear resistance of the samples. Depth-sensing nanoindentation measurements were performed for the elastic modulus and nanohardness of the DLC coatings.

Room temperature emissitivity was measured to study the IR range optical behavior of the DLC coatings using a Benchtop spectral emissometer that can acquire radiance, reflectance, and transmittance simultaneously. The *I–V* characteristics and the influence of light on the conduction of several films were analyzed. The low temperature resistivity as a function of cryogenic temperature was recorded to investigate the transport behavior of the samples.

3. Results and discussion

3.1. Surface condition and microstructure of the DLC coatings

Profilometry on the single-layer doped and undoped DLC coatings deposited for 40 min showed consistently that the coating thickness is in the range of 400–600 nm. RBS results as well as XPS analyses both showed that the atomic fraction of the dopants is less than 5% for most DLC coatings. Particularly for metals such as Cu and Ag, the atomic fraction is smaller than 3% [25]. Composition of the DLC coatings can be changed through changing either the position of the laser beam on the target or the size of the metal piece. This will change the perimeter of the circle made by the laser beam on the target surface and the fraction of ablated metal in the circle is therefore changed.

Observation of the surface morphology of the doped DLC coatings showed that Cu and Ag give much less particulate density than Ti and Si do [25]. The geometry and size of the particulates suggest that they were formed out of condensed liquid droplets, typically found in pulsed laser ablation of most materials. The surface of pure DLC coatings has been found to be atomically smooth via atomic force microscopy [12].

Fig. 1 is the Raman spectra of pure DLC, DLC doped with Ti, Cu and Si, respectively. These spectra are

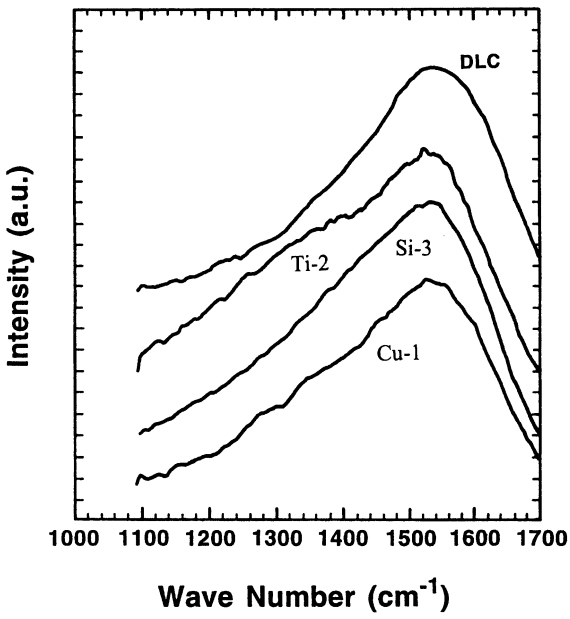

Fig. 1. Raman spectra of a pure DLC coating, and those containing copper, titanium and silicon.

typical of DLC films, with a broad peak centered approximately 1510–1580 cm^{-1}, which could be understood based on the G-band of crystalline graphite, and a shoulder part located at approximately 1350 cm^{-1}, associated with the disorder-allowed zone edge mode of poly-crystalline graphite (D-band). It appears that the DLC film doped with Ti shows more asymmetry and an increased D band in the Raman spectrum as compared with other specimens. There is a general tendency in Fig. 1 that all the peak positions of the G-band of the doped samples have been shifted toward smaller wave numbers. This shift was used to analyze the internal stress reduction in the doped DLC coatings [25].

The effect of the dopants on the Raman spectra of DLC coatings may be understood on the basis of the electronic structure of the dopants themselves, and their interaction with carbon atoms. For example, since the *d* shell of copper is fully occupied and it has been recognized that Cu has little chemical bonding with carbon, it might be expected that Cu would not contribute much to changing the short-range environment of the DLC either. The outer shell electronic structure of a titanium atom is $3d^2 4s^2$, and it might be envisaged that this shell configuration could contribute to the change of short-range electronic structure of DLC and thus give rise to the change in the Raman spectrum. XPS analyses on these samples demonstrated that Cu has no bonding with carbon, while Ti–C bonding and formation of titanium carbide was detected in the DLC coating containing Ti [25,27].

RDF analysis enables us to obtain information of the first and second coordination spheres, such as the dis-

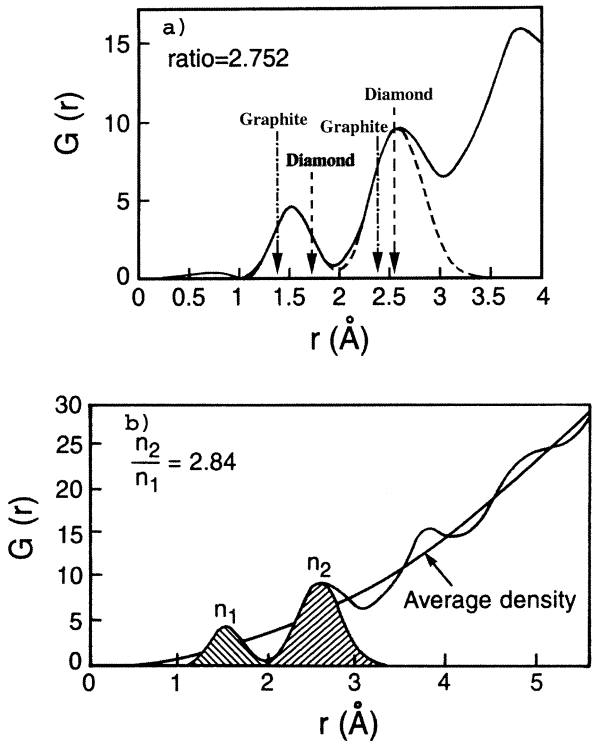

Fig. 2. RDF of pure DLC (a) and DLC+1.2 at.% Cu (b). For comparison, the first and second nearest-neighbor distances of diamond are 1.544 and 2.512 Å, and the ratio of the first to the second shell coordination number is 3, while the first and second nearest-neighbor distance of graphite are 1.42 and 2.45 Å, respectively, and the ratio of the first to the second shell coordination number is 2.

tance of the first and second nearest neighbors, and the coordination numbers, etc. [31]. In the case of DLC, since it has both four- and threefold coordination, the first and second coordination spheres in the RDF should have coordination numbers between those of graphite [3,6] and those of diamond [4,12].

Fig. 2a shows the RDF calculated from the electron diffraction data of pure DLC. The first and second nearest-neighbor distances as obtained from the RDF analysis are 1.51 and 2.52 Å, respectively. The ratio of the second shell coordination number to the first shell coordination number is approximately 2.75. Fig. 2b shows the RDF for the DLC coating with 1.2 at.% Cu. For this sample, the first and second nearest-neighbor distances are 1.50 and 2.54 Å, respectively, while the ratio of the second shell coordination number to the first shell coordination number is approximately 2.84. The structural data imply that the presence of copper atoms does not change the short-range environment significantly.

3.2. Mechanical and tribological behavior of the DLC coatings

It was found that all the doped DLC coatings stick well to the substrate [25]. On the other hand, in the case of the pure DLC coating, severe buckling was observed. Usually, buckling would not spread over the whole surface but start from edges of the specimen. The sinusoidal shape of the buckling pattern could be clearly established, which indicates that it is due to the relief of internal compressive stress in the coating. Also, buckling is dependent on both the internal compressive stress in the film and the stress at the film–substrate interface. For DLC coatings, one of the critical variables is the coating thickness since the stress level in the coating itself scales with coating thickness.

It is noted that the buckling phenomenon is absent in all the doped DLC coatings [25,28]. It appears that the most likely explanation is that the presence of dopants can help reduce the internal compressive stress in the DLC coatings. In order to have a better understanding of how the presence of dopants enhances the adhesion of the DLC coatings, we carried out qualitative scratch tests on pure DLC and some doped DLC coatings. To do this, we used a constant normal load of 10 g for all the coatings and drew the indenter across the coatings. Fig. 3 shows the scratches made on different DLC coatings. In the case of pure DLC (Fig. 3a), the coating is easily stripped off from the substrate, indicating poor

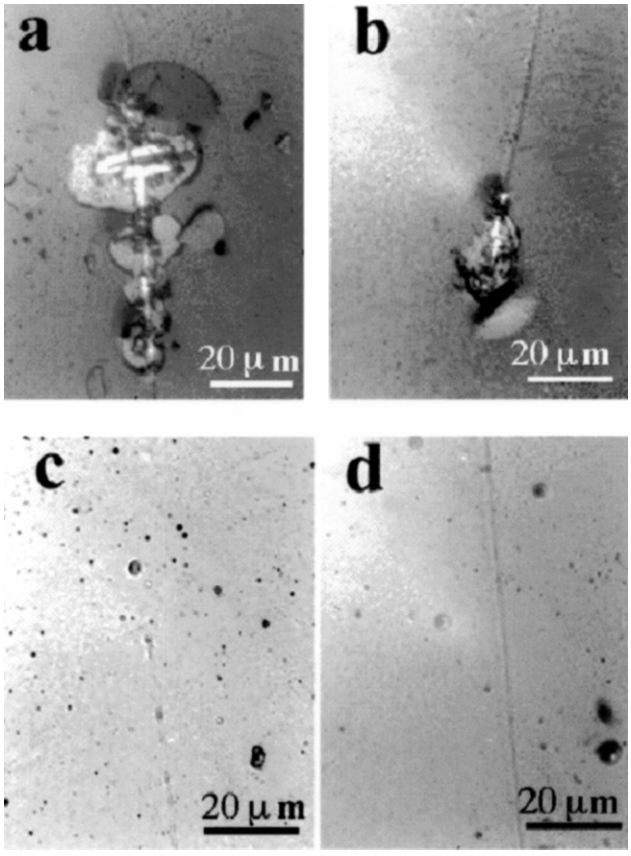

Fig. 3. Optical micrographs of scratches made on pure DLC (a), DLC+Cu (b), DLC+Ti (c) and DLC+Si (d), showing different adhesion properties of these coatings.

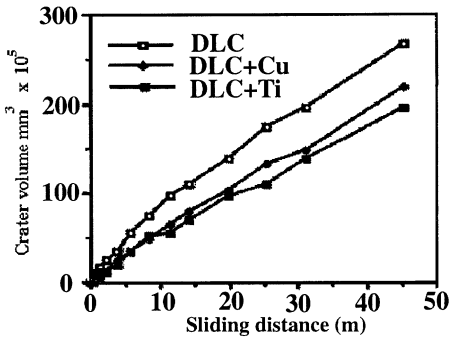

Fig. 4. Wear test results for pure DLC, DLC + Cu, and DLC + Ti coatings.

adhesion. This is consistent with the optical microscopy studies of the buckling patterns of pure DLC coating [25]. In all the doped DLC samples, the coatings adhere well to the substrate (Fig. 3b–d). This is particularly true for DLC films containing Ti (Fig. 3c) and Si (Fig. 3d).

Another important mechanical behavior for tribological applications is wear resistance. In our study, we use a 'crater grinding method' based on a micro-abrasion mechanism [27] to acquire the wear resistance of the DLC coatings. A nominal load of 5 g was applied to create the craters. Fig. 4 shows the wear test results for the pure DLC, DLC + Cu, and DLC + Ti coatings on silicon. It is found from Fig. 4 that Achard's law [32] is satisfied for these specimens. Improvement of wear resistance of the DLC coatings through incorporation of metal is significant, especially during the initial stages of the wear test. It is also observed that the effect of titanium is stronger than that of copper. One possible reason may be that titanium is a strong carbide former and it produces relatively stronger bonding with carbon in the coating, whereas Cu is a very weak carbide former and it is doubtful whether it exists in carbide. This is in accordance with our XPS studies as described elsewhere [25,27].

The improvement of wear resistance by incorporating foreign atoms into the DLC coatings is consistent with the enhancement of adhesion of these coatings by doping. It appears based on our discussions that this improvement most probably results from reduction in the internal compressive stresses.

We have measured the nanohardness (H) and Young's modulus (E) as a function of indentation depth, using a depth-sensing nanoindentation technique. The values for H and E for pure DLC are 240 and approximately 40 GPa, respectively, indicating good coating quality in terms of nano-mechanical properties. In comparison to the undoped DLC, both E and H for the Cu and Ti doped DLC coatings are slightly reduced. This slight cost in hardness and elastic modulus has been compensated for by the reduction of the internal compressive stress, which in turn enhances the tribological performance of the coatings.

The reduction of internal compressive stress through incorporation of dopants might be understood by invoking the atomic structure of DLC. In the case of the widely accepted continuous rigid random network (CRN) model, the reduction of the internal compressive stress through the in situ introduction of dopants can then be explained on the basis of the effect of these dopants on the CRN of DLC. Transition metals like Cu, Ti and Ag are usually more compliant as compared to covalently bonded materials like DLC. The substitution of metal dopants for carbon atoms in the CRN may be able to accommodate or take up the strain by distortion of the electron density distribution since the outer shell electrons of the transition metals are loosely bound to the atom. The effect of Si can also be interpreted by the same token. However, detailed theoretical modeling is still needed to elucidate the underlying mechanism that leads to the stress reduction. Also important is the information of how the dopant atoms are distributed in the CRN of DLC.

3.3. Electrical and IR range optical properties of the DLC coatings

Four-probe measurements showed that the resistance of the DLC films does not change linearly with dopant concentration, in agreement with what has been reported [33]. Amorphous semiconductors usually have all states localized, and their conduction exhibits hopping, especially variable-range hopping mechanisms. The hopping probability can be expressed as [34]

$$w_{ij} = w_0 \exp\left(-\frac{2R}{\lambda} - \frac{W}{kT} \right), \tag{1}$$

where w_0 is a constant, R is the distance the electron crosses by tunneling in one hopping event; λ is a measure of the extent of the state (localization length), W is the thermal activation energy, k is Boltzmann constant, and T is absolute temperature. Eq. (1) indicates that the hopping probability and thus the conductivity of the materials will be increased with decreased R. When the concentration of foreign atoms that can contribute to localized states is increased, the distance that the electron will cross over one tunneling event would be smaller, leading to a reduced resistivity. When the concentration of these atoms is increased to such a level that continuous channels might be formed for the transport of electrons, the material could essentially behave like metallic materials.

DLC films containing copper exhibit p-type conduction, as pure DLC. Generally, Cu has been reported to act as an acceptor in most semiconductors [35]. For example, it has three acceptor levels in crystalline

silicon. Therefore, it is not surprising that DLC coatings containing Cu also show p-type conduction.

Measurements of the *I–V* characteristics of the pure DLC and those containing dopants showed that, all the coatings except the one containing Ti form a Schottky contact with the measuring probe [26]. The DLC + Ti sample simply exhibits metallic conduction as a resistor, with its *I–V* curve following Ohm's law. This can in part be understood in connection with the XPS observation that Ti–C bonding is present in the film. Ti–C bonding is essentially metallic and its presence might greatly enhance the conduction of the film by increasing the density of states near the Fermi level. It was also observed that light has a strong effect on electrical conduction of the DLC coatings [26,29].

The conductivity of the DLC + 1.2 at.% Cu sample as a function of temperature exhibits two regimes. The first regime corresponds to higher temperature conduction close to room temperature, and the second, to low-temperature conduction. The data for the low-temperature regime can be well fit by the relation

$$\sigma \propto \exp\left(-\frac{B}{T^{1/2}}\right), \tag{2}$$

where B is a constant. This temperature dependence of conductivity is different from the famous Mott–Davis law [36], but it has also been observed in other disordered material systems. This behavior can be understood on the basis of the theory developed by Efros and Shklovskii [37], who derived the $\sim T^{-1/2}$ dependence by considering the long-range Coulomb interactions between the localized states. Likewise, in the DLC coating that has a small fraction of dispersed Cu atoms, the copper atoms are envisaged as Coulomb interaction centers, which results in the $\sim T^{-1/2}$ behavior.

Since one of the applications of DLC is for protective coatings for IR windows, it should be important to study the effect of foreign atoms on the IR range optical properties. Measurements of emissivity were performed on pure DLC coatings and those with dopants. Emissivity is defined as the ratio of the radiance of a given object to that of a black body at the same temperature, and for the same spectral and directional conditions. It is a function of wavelength and temperature. There are generally three contributions to the emittance of a semiconductor, i.e. band-to-band transitions, free carriers, and phonons (lattice vibrations). In the case of defect-free crystalline semiconductors such as intrinsic silicon, the three contributions are distinct from one another at low temperatures where the concentration of free carriers is still low. The emissivity increases abruptly when the photon energy exceeds the band gap. Fig. 5 shows emittance of DLC and DLC + 1.4 at.% Cu specimens measured near room temperature. The emittance spectrum exhibits three regimes. The first regime

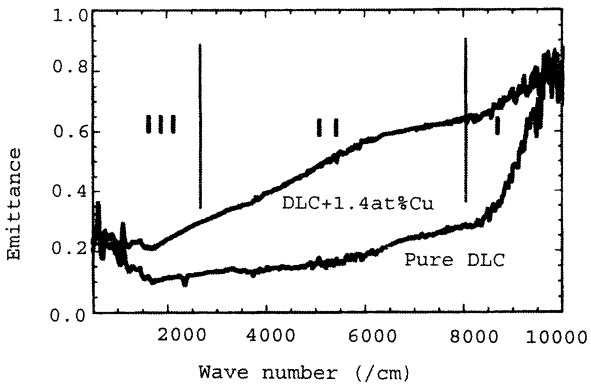

Fig. 5. IR range emissivity spectra of pure DLC, and DLC + Cu (1.4 at.% Cu) coatings, showing the emittance (%) as a function of wave number. Three regimes are indicated in the specimen for pure DLC.

corresponds to large wave numbers (higher photon energies) that show high emittance. Though DLC films prepared by 248-nm excimer laser with high laser fluence ($\sim$10 J/cm^2) have been reported to have a band gap of $\sim$1.5 eV, Dikshit et al. [33] reported a value close to 1.0 eV on DLC films prepared under the same laser fluence as the present work. We may therefore attribute the first regime to band-to-band transitions. Apart from this, however, in the case of amorphous semiconductors, there are a large number of localized states, especially close to the band edges. We might expect that these localized states would also contribute to emittance. This is indeed what happens to DLC where no sharp transitions are observed in the emittance spectrum. Instead, gradual changes are present. The second regime is from free carriers, while the third regime of wavenumber close to 10^3 cm^{-1} is due to phonon contribution. When the specimen is doped, this contribution from free carriers can be enhanced significantly. It was found that incorporation of a small amount of Si into DLC coatings does not change the general features of the emissivity and transmittance spectra [26,29]. Instead, it was found to contribute slightly to the localized state part, and also contributes a little to the free carriers part. The emittance of DLC containing a small fraction of metallic elements shows a significant increase in the whole range of measurement, while the transmittance in the IR range is considerably decreased so that the coating is almost opaque. The effect of titanium is much more profound in this respect. Ti-incorporated DLC coatings behave almost as a black body, where the transmittance just goes to zero. Free carriers suppress all contribution from band-to-band transitions, from localized states and from phonons. In other words, the emitted radiation from other contribution might have been absorbed before it reaches the specimen surface.

3.4. Application of functionally gradient design for DLC coatings

In order to produce even thicker DLC coatings with reduced internal compressive stress and improved adhesion, we have adopted functionally gradient (FG) design by using the advantage of PLD. The alloy element was incorporated during the PLD process, with the concentration of the alloy element decreased away from the coating/substrate interface. Silver, copper and titanium were chosen as alloy elements to be incorporated into the composite layer. Three layers of different alloy element contents were deposited for 30 min each, and the final top pure DLC layer was deposited for 30 min.

It was found by optical profilometer that the thickness of the FG diamond-like carbon coatings is from 1.4 to 1.6 μm, depending on the type of alloy element incorporated below the pure DLC layer. Fig. 6 is the nano-hardness (a) and Young's modulus (b) as a function of indentation depth for a single layer of pure DLC deposited with 309-mJ laser energy as well as FG DLC coatings. Values of ~420 GPa for Young's modulus and ~54 GPa for nano-hardness are obtained for pure thin DLC films. As pointed out by Ferrari et al. [38], nano-indentation is seen to underestimate E for Ta–C. Surface Brillouin scattering measurements yielded E of 750 GPa for FCVA deposited DLC films which give nano-indentation results similar to ours. The constraint-counting network [39] predicts that Young's modulus should depend on mean-atomic coordination Z as

$$E = E_0(Z - Z_0)^{1.5}, \quad (3)$$

where Z_0 is the critical coordination, below which the networks have zero rigidity. The theoretical value of Z_0 was given to be 2.4, and Ferrari et al. [38] obtained a value of 2.6 for Z_0 based on experimental observations. Extrapolation of surface Brillouin scattering measurements [38] and molecular dynamics simulation of a 100% sp^3 DLC [40] yielded a value of 480 GPa for E_0. Therefore, from nano-mechanical measurements and Eq. (3), a conservative estimation of sp^3 fraction can be made using the relationship between sp^3 fraction and the coordination number, which is $Z = 3 + sp^3$. Therefore, for the pure DLC deposited with 309-mJ laser energy, the sp^3 fraction is conservatively estimated to be ~51%.

The nano-hardness of DLC/DLC+Ag/…/Si is approximately 60 GPa, which is close to that of crystalline diamond (~100 GPa), and much higher than that of silicon carbide (~35 GPa). The nano-hardness of DLC/DLC+Cu/…/Si FG coating is close to ~50 GPa, also much higher than that of silicon carbide. The FG coating that shows the lowest nano-hardness is DLC/DLC+Ti/…/Si, which is only ~40 GPa, still slightly higher than that of silicon carbide.

FG coating of DLC/DLC+Ag/…/Si exhibits the highest value of Young's modulus. From the elastic

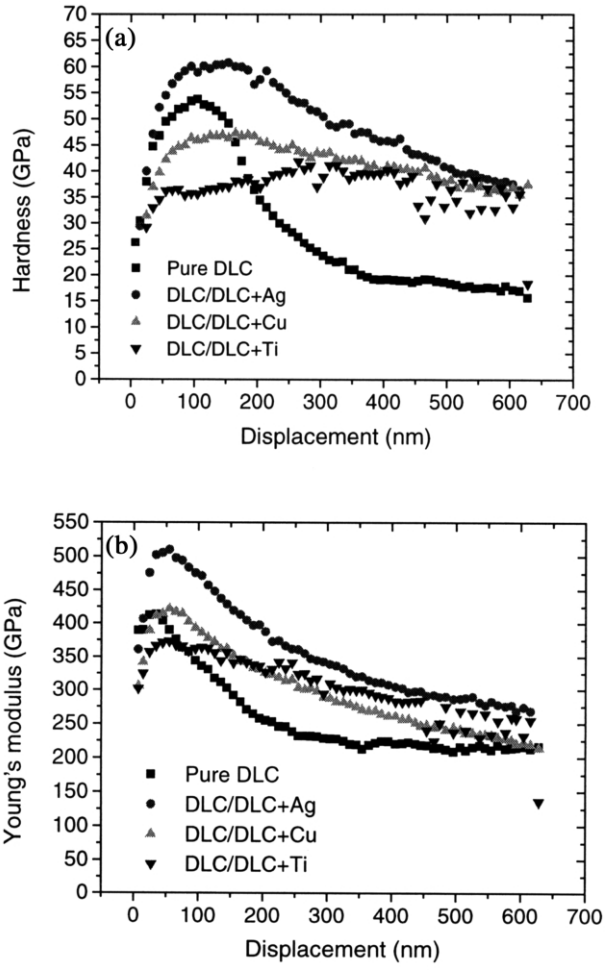

Fig. 6. Nano-hardness (a) and Young's modulus (b) of pure DLC layer produced by 309 mJ laser energy (the film thickness is approx. 250 nm) and of functionally graded DLC coatings with Ag, Cu and Ti as the alloy elements. Notice the difference in the effect of the three different alloy elements (Ag, Cu and Ti) and decrease of substrate effect as compared to pure, thin DLC film.

modulus and Eq. (3), we can estimate the sp^3 fraction of the pure DLC layer to be ~64%. For DLC/DLC+Cu/…/Si FG coating, the estimated sp^3 fraction for the top pure DLC layer is approximately 53%, and for DLC/DLC+Ti/…/Si FG coatings, it is approximately 45%. Our previous work showed that incorporation of Ti into the DLC coatings reduces Young's modulus more than Cu does [25]. Neither copper nor silver form strong chemical bonds with carbon, and the existence of these elements may only help the relaxation of the internal compressive stress.

One of the advantages of FG DLC coatings is the decrease of the substrate effect during the nano-mechanical probing process, as reflected from the nano-indentation measurements. This can be established by comparing the curves in Fig. 6. In the case of a pure DLC coating that is approximately 250 nm thick, the substrate effect sets in at the very early phase of nano-

indentation. While in the case of thick FG DLC coatings, the situation is significantly improved. Of course, the major advantage of the FG DLC design is that it allows us to produce much thicker DLC coatings than traditional approaches.

Voevodin et al. [41,42], also produced FG DLC coatings, but with a different route. They used a hybrid of magnetron sputtering and PLD multi-source schemes to deposit crystalline Ti, TiC and amorphous DLC films, with a total thickness of 2–3 μm and hardness of approximately ~65 GPa. It is reasonable to expect that FG DLC design will be advantageous at least for tribological applications.

4. Summary and concluding remarks

Functional diamond-like carbon coatings with reduced internal compressive stress and improved adhesion have been successfully prepared by pulsed laser ablation. The DLC coatings contain a small fraction of more compliant atoms such as transition metals. It was found that these DLC coatings exhibit significantly improved nanomechanical and tribological performance. Microstructural and atomic structural analyses showed that the DLC coatings maintain the short-range environment of mostly tetrahedrally bonded amorphous carbon. Electrical and IR range optical measurements were also conducted to study the effect of foreign atoms on the properties. It was demonstrated that functionally gradient design could be applied for the preparation of thick, superhard, adherent DLC coatings by pulsed laser ablation.

Acknowledgements

This work has been sponsored by National Science Foundation through National Science Foundation Center for Advanced Materials and Smart Structures, jointly affiliated with North Carolina A&T State University and North Carolina State University. The authors would like to thank Dr A.K. Sharma for technical assistance and many helpful discussions through out this research.

References

[1] Q. Wei, J. Narayan, Int. Mater. Rev. 45 (2000) 133.
[2] P.W. Atkins, Physical Chemistry, 5th ed., W.H. Freeman and Company, San Francisco, 1994.
[3] J. Robertson, Prog. Solid State Chem. 21 (1991) 199.
[4] A.A. Voevodin, M.S. Donley, Surf. Coat. Technol. 82 (1996) 199.
[5] W.I. Milne, J. Non-Cryst. Solids 198-200 (1996) 605.
[6] K. Enke, Mater. Sci. Forum 52-53 (1990) 559.
[7] M.P. Siegal, W.I. Milne, J.I. Jaskie (Eds.), Covalently Bonded Disordered Thin-Film Materials, MRS Symp. Proc. 498 (1998).
[8] J. Krishnaswamy, A. Rengan, J. Narayan, K. Vekom, C.J. McHorgue, Appl. Phys. Lett. 54 (1989) 2455.
[9] T. Sato, S. Furuno, S. Ifuchi, M. Hanabusa, Jpn. J. Appl. Phys. 26 (1987) 1487.
[10] D.L. Pappas, K.L. Saenger, J. Bruley, W. Krakow, J.J. Cuomo, J. Appl. Phys. 71 (1992) 5672.
[11] E.A. Rohlfing, J. Chem. Phys. 89 (1988) 6103.
[12] Q. Wei, J. Sankar, A.K. Sharma, Y. Yamagata, J. Narayan, J. Vac. Sci. Technol. A19 (2001) 311.
[13] M. Chhowalla, Y. Yin, G.A.J. Amaratunga, D.R. McKenzie, Th. Frauenheim, Diamond Relat. Mater. 6 (1997) 207.
[14] J. Kulik, Y. Lifshitz, G.D. Lempert, J.W. Rabalais, D. Marton, J. Appl. Phys. 76 (1994) 5063.
[15] D. Nir, Thin Solid Films 146 (1984) 27.
[16] M. Weiler, S Sattel, T. Giessen, K. Ehrhardt, Phys. Rev. B53 (1996) 1594.
[17] J.P. Sullivan, T.A. Friedmann, A.G. Baca, J. Electron. Mater. 26 (1997) 102.
[18] P. Koidl, C. Wild, B. Dischler, J. Wagner, M. Ramsteiner, Mater. Sci. Forum 52-53 (1989) 41.
[19] D.R. Mckenzie, D. Muller, B.A. Pailthorpe, Phys. Rev. Lett. 67 (1991) 773.
[20] M. Crischke, K. Bewilogua, K. Trojan, H. Demigen, Surf. Coat. Technol. 74-75 (1995) 739.
[21] M.D. Bentzon, K. Mogensen, J.B. Hansen et al., Surf. Coat. Technol. 68-69 (1994) 651.
[22] J. Narayan, R.D. Vispute, K. Jagannadham, J. Adhes. Sci. Technol. 9 (1995) 753.
[23] T.A. Friedmann, J.P. Sullivan, J.A. Knapp et al., Appl. Phys. Lett. 71 (1997) 3820.
[24] A.C. Ferrari, B. Kleinsorge, N.A. Morrison, A. Hart, V. Stolojan, J. Robertson, J. Appl. Phys. 85 (1999) 7191.
[25] Q. Wei, R.J. Narayan, A.K. Sharma, J. Sankar, J. Narayan, J. Vac. Sci. Technol. A17 (1999) 3406.
[26] Q. Wei, J. Sankar, A.K. Sharma, S. Oktyabrsky, J. Narayan, R.J. Narayan, J. Mater. Res. 15 (2000) 633.
[27] Q. Wei, R.J. Narayan, J. Narayan, J. Sankar, A.K. Sharma, Mater. Sci. Eng. B53 (1998) 262.
[28] Q. Wei, R.J. Narayan, A.K. Sharma, J. Sankar, J. Narayan, Covalently Bonded Disordered Thin Film Materials, MRS Symp. Proc. 498 (1998) 61.
[29] Q. Wei, R.J. Narayan, A.K. Sharma, J. Sankar, S. Oktyabrasky, J. Narayan, Processing and Properties of Vapor Deposited Coatings, MRS Symp. Proc. 555 (1999) 303.
[30] Q. Wei, R.J. Narayan, A.K. Sharma, J. Sankar, J. Narayan, Thin Films: Stresses and Mechanical Properties VII, MRS Symp. Proc. 505 (1998) 331.
[31] D.J.H. Cockayne, D.R. McKenzie, Acta Crystal. A44 (1988) 870.
[32] J.F. Achard, J. Appl. Phys. 24 (1953) 981.
[33] S.J. Dikshit, P. Lele, S.B. Ogale, S.T. Kshirsagar, J. Mater. Res. 11 (1996) 2236.
[34] O. Madelung, Introduction to Solid State Theory, Springer, Berlin, 1996.
[35] A.G. Milnes, Deep Impurities in Semiconductors, John Wiley & Sons, New York, 1973.
[36] N.F. Mott, E.A. Davis, Electronic Processes in Non-crystalline Materials, 2nd ed., Clarendon Press, Oxford, UK, 1979.
[37] A.L. Efros, B.I. Shklovskii, J. Phys. C: Solid State Phys. 8 (1975) L49.
[38] A.C. Ferrari, J. Robertson, M.G. Beghi, C.E. Bottani, R. Ferulano, R. Pastorelli, Appl. Phys. Lett. 75 (1999) 1893.
[39] H. He, M.E. Thorpe, Phys. Rev. Lett. 54 (1985) 2107.
[40] P.C. Kelires, Phys. Rev. Lett. 73 (1994) 2460.
[41] A.A. Voevodin, M.A. Capano, S.J.P. Laube, M.S. Donley, J.S. Zabinski, Thin Solid Films 298 (1997) 107.
[42] A.A. Voevodin, J.S. Zabinski, Diamond Relat. Mater. 7 (1998) 463.